The influence of water on the reduction and reoxidation of ceria

Celestino Padeste[a], Noel W. Cant[b] and David L. Trimm[a]

[a] *School of Chemical Engineering and Industrial Chemistry, University of New South Wales, PO Box 1, Kensington, NSW 2033, Australia*
[b] *School of Chemistry, Macquarie University, NSW 2109, Australia*

Received 3 December 1992; accepted 13 January 1993

Two different samples of ceria have been characterized by temperature programmed reduction in carbon monoxide (CO-TPR), surface area determination and transmission electron microscopy (TEM). The much higher reducibility at temperatures below 550°C of a sample prepared by decomposition of cerium carbonate, compared to a commercial ceria, was attributed to the much lower crystallinity. When this ceria, in the partly reduced state, was brought in contact with water vapour, it was readily reoxidised with evolution of hydrogen. The oxygen storage capacity of this sample, determined in cycling experiments, was considerably lowered by the presence of water.

Keywords: Ceria reduction; oxygen storage capacity; CO-TPR; XPS; TEM

1. Introduction

Since ceria was found to improve the performance of three-way car exhaust catalysts, many investigations have been carried out to elucidate the reasons for the improvement. Ceria has been found to stabilize the high surface area Al_2O_3 support [1], to promote the reduction of precious metals [2] and to stabilize them in the reduced state [1–3], to promote water–gas shift and steam reforming reactions as well as NO reduction [2,4] and to contribute to sulphur storage [1]. One of the most popular interpretations of the role of ceria in exhaust catalysts is that the oxide acts as an oxygen storage component. During periods in which the engine runs at rich fuel/air ratios, cerium would be partially reduced from oxidation state +IV to +III according to the reaction

$$CeO_2 + x \text{ red} \rightleftharpoons CeO_{2-x} + x \text{ ox}, \quad (1)$$

where "red" is a reducing agent such as H_2 or CO and "ox" is the oxidation product [4–7]. During periods of lean fuel/air ratios, when excess oxygen is present and NO is produced in relatively high amounts, the ceria would be reoxidised by O_2, or by NO [6,7] according to

$$CeO_{2-x} + \tfrac{1}{2}xO_2 \rightleftharpoons CeO_2 \tag{2}$$

and

$$CeO_{2-x} + xNO \rightleftharpoons CeO_2 + \tfrac{1}{2}xN_2\,. \tag{3}$$

The fact that cerium +IV in aqueous solutions is a strong oxidising agent often leads to the assumption that the reduction of Ce^{+IV} in CeO_2 should be relatively facile, especially at elevated temperatures.

If the thermodynamics of the Ce–O-system is examined, the situation appears rather different. CeO_2 crystallizes in a fluorite structure in which each cerium ion is coordinated by eight oxygen neighbours. This coordination apparently stabilizes Ce^{+IV} ions and makes reduction unfavourable. Table 1 summarizes results from calculations of the equilibrium partial pressures of oxygen over partially reduced ceria based on equilibration in hydrogen/water mixtures [8]. These results indicate that pure ceria is significantly reduced only under strongly reducing conditions. In car exhaust gases however, the conditions are never strongly reducing, because there is always, even at rich fuel/air ratios, an excess of potentially oxidising gases (mainly H_2O and CO_2) present.

The present studies are focussed on the behaviour of unsupported pure ceria under reducing and oxidising conditions in presence of water.

2. Experimental

Cerium(IV) oxide (Aldrich, 99.9%) and cerium(III) carbonate hydrate (Aldrich, 99.9%) were used as starting materials. For the reduction and reoxidation

Table 1
Equilibrium partial pressures of oxygen over oxygen deficient ceria at various temperatures, determined in H_2O/H_2 mixtures at atmospheric pressure (from ref. [8])

Temperature (°C)	Stoichiometry	p_{H_2O} (mm Hg)	p_{O_2} (atm)[a]
600	$CeO_{1.996}$	15.9	2.2×10^{-27}
600	$CeO_{1.993}$	0.86	2.0×10^{-30}
600	$CeO_{1.845}$	0.28	2.0×10^{-31}
600	$CeO_{1.830}$	0.09	2.0×10^{-34}
700	$CeO_{1.986}$	15.9	7.2×10^{-25}
700	$CeO_{1.838}$	0.58	9.8×10^{-28}
700	$CeO_{1.830}$	0.09	2.2×10^{-27}
805	$CeO_{1.868}$	15.9	8.7×10^{-22}
800	$CeO_{1.813}$	0.93	7.6×10^{-25}
800	$CeO_{1.742}$	0.09	6.7×10^{-27}

[a] Calculated from p_{H_2O} and p_{H_2}.

studies, the powder samples were pressed to pellets, crushed with a razor blade, and sieved to 100–400 μm. The reactions were carried out in a flow system in which gas mixtures were passed at 40 ml/min over 100–300 mg samples fixed in a glass tube using glass wool. The tube was placed in a furnace which was programmed at a rate of 10°C/min up to 550°C. Changes in the composition of the product gas were determined using a VG SX300 quadrupole mass spectrometer.

Surface areas were determined by single point nitrogen adsorption at liquid nitrogen temperature from a 30% N_2/He mixture in a flow system equipped with a thermal conductivity detector.

The XPS spectra were recorded on a Kratos XSAM AXIS 800pci spectrometer equipped with a concentric hemispherical analyzer which was run in the fixed transmission mode at pass energy 40 eV. A Mg K_α X-ray source was used at 180 W. The base pressure of the system was less than 10^{-9} Torr. The samples were ground to fine powders and suspended in acetone. The resulting slurry was deposited on a stainless steel sample holder. After evaporation of the solvent, the powder was bound to the holder sufficiently strongly to be introduced in the vacuum system. The energy scale of the spectra of non-conducting samples was calibrated against the C 1s line of adventitious carbon at $E_B = 285$ eV. Some samples were thermally pretreated in vacuum (less than 10^{-4} Torr) in a chamber attached to the spectrometer and subsequently transferred into the main chamber of the instrument without contact with air. A dosing system allowed admission of water of pressures up to 5×10^{-4} Torr into a turbo-pumped preparation chamber with a base pressure of less than 5×10^{-7} Torr.

The morphology and microstructure of the different ceria samples were studied on a Jeol 2000 SX transmission electron microscope. The samples were ground to fine powders in an agate mortar, suspended in ethanol and deposited on copper grids covered with amorphous carbon.

3. Results and discussion

3.1. THERMOPROGRAMMED REDUCTION (TPR) OF DIFFERENT CERIA SAMPLES

Most studies of the reduction of ceria have been performed using hydrogen as a reducing agent, even though carbon monoxide might be more important for reductions in exhaust systems. The reduction of ceria by hydrogen depends greatly on characteristics of the sample such as specific surface area and crystallite size [5,9]. Reduction below 500°C is more pronounced for samples with high surface area, and is therefore assigned to surface reduction. On the other hand, bulk reduction at higher temperatures (600–900°C) depends little on the specific surface area [5].

In this study, CO was used to investigate the reduction characteristics of two different ceria samples, a pure Aldrich-CeO_2 (ceria-A) and a sample prepared from cerium(III) carbonate by decomposition in 5% O_2/He at 550°C for 15 min directly

before use (ceria-C). Under these conditions, the cerium carbonate is transformed to cerium(IV) oxide [10]. Fig. 1 shows the formation of CO_2 during TPR of the two samples in the range from room temperature up to 550°C in 2% CO/He. Simultaneous measurements of CO consumption and CO_2 production were in good agreement in all cases, indicating that oxidation of CO by oxygen from the sample was the major process taking place. Only the results from the CO_2 formation are shown in fig. 1. For both samples, the reduction was similar when used fresh or reduced and reoxidised in O_2/He, indicating a high degree of reversibility of the reaction.

The difference between the two samples is remarkable. With ceria-A the reduction starts at lower temperatures, but at elevated temperatures the reduction of ceria-C is much greater. The degree of reduction was estimated from the oxygen consumption during reoxidation at 400°C in a 2% O_2/He mixture. The calculated extent of reduction of Ce^{+IV} to Ce^{+III} was 1–2% for ceria-A compared to 10–15% for ceria-C. Surprisingly the difference in surface area was much less (15 m^2/g and 30 m^2/g for ceria-A and ceria-C respectively). This parameter can, therefore, only account for a part of the difference in reduction behaviour.

Transmission electron microscopy revealed pronounced differences in the crystallinity of the two samples (fig. 2). Ceria-A shows a heterogeneous distribution of crystallites of two different sizes, i.e. most particles are in the range of either 15 or 70 nm in diameter. The corresponding electron diffraction patterns indicate very high crystallinity for the particles of both sizes. For ceria-C, very low crystallinity is

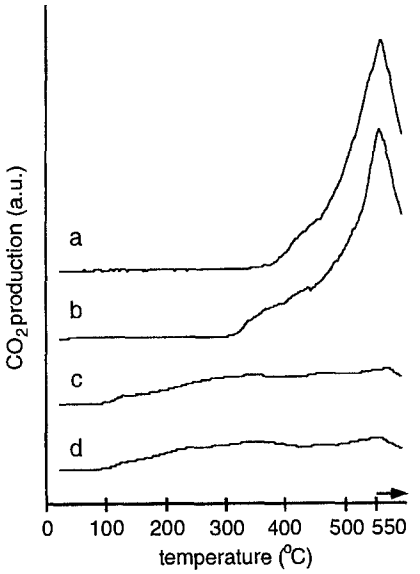

Fig. 1. Carbon dioxide production during TPR of ceria in a 2% CO/He mixture (40 ml/min). Heating rate: 10°C/min. Samples: 240 mg ceria-C, (a) freshly prepared from cerium carbonate and (b) after reduction and reoxidation; 220 mg ceria-A, (c) fresh and (d) after reduction and reoxidation. Reoxidation conditions: 2% O_2/He, 40 ml/min, 400°C, 10 min.

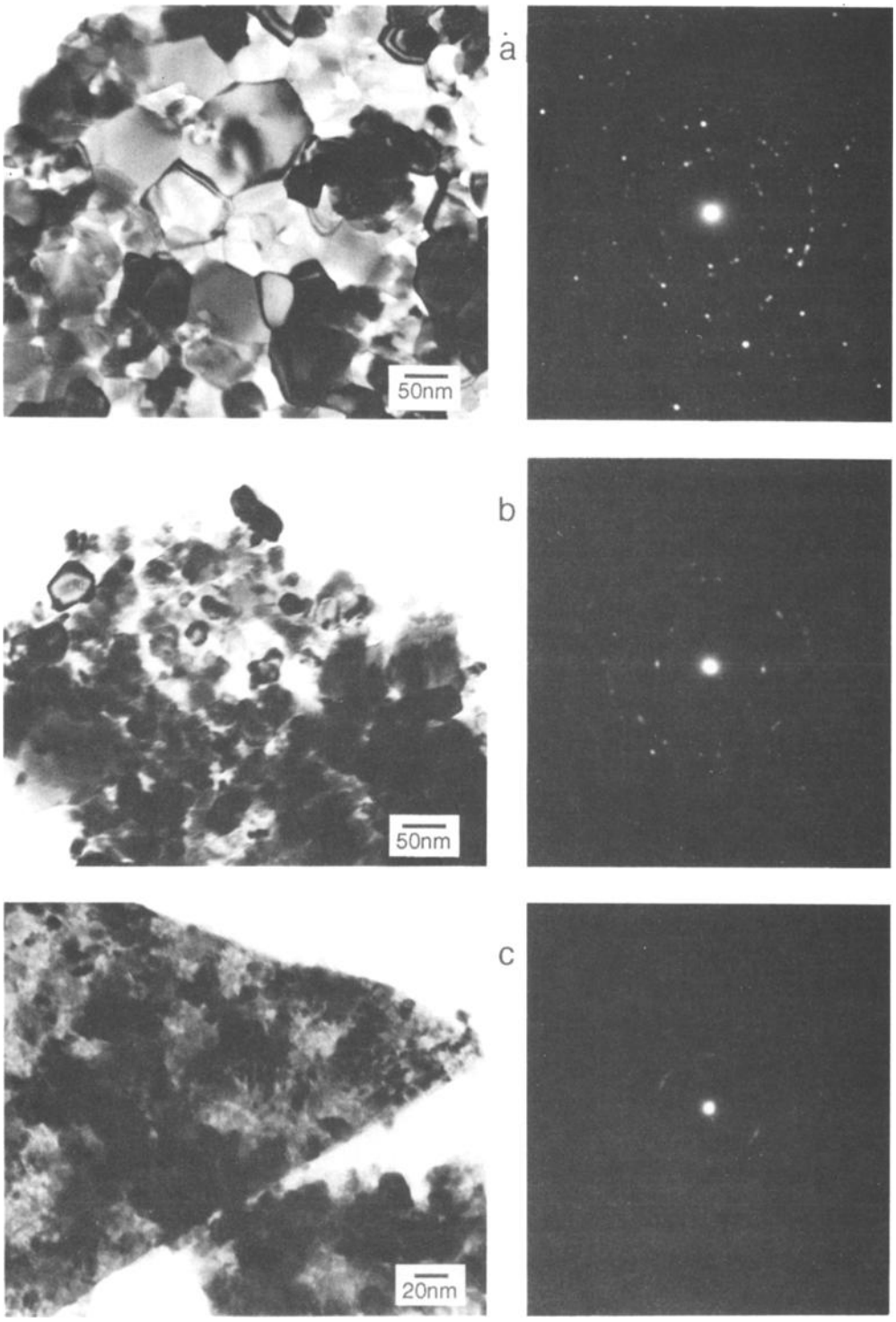

Fig. 2. Transmission electron micrographs and electron diffraction patterns of two areas of ceria-A (a and b) and ceria-C (c).

indicated by the diffraction pattern, where a set of diffraction rings, rather than point reflections was found. The micrograph of ceria-C shows big conglomerates of very small particles. A high resolution micrograph of this sample (fig. 3) revealed crystalline microdomains with a diameter of less than 10 nm. The sharp edges of some of the conglomerates (fig. 2c) originate most probably from much larger crystallites in the parent material. The pseudomorphous character of the decomposition product explains a relatively low surface area, even though the crystallinity of the sample is very low.

A possible interpretation of the TPR results is that the reduction of ceria-A in the temperature range investigated is largely restricted to the surface, while bulk reduction at relatively low temperatures is favoured by the high amount of crystal imperfections in ceria-C.

3.2. REOXIDATION OF REDUCED CERIA BY WATER

3.2.1. Reoxidation at elevated temperature

The reoxidation of oxygen deficient ceria by water was determined at 550°C on

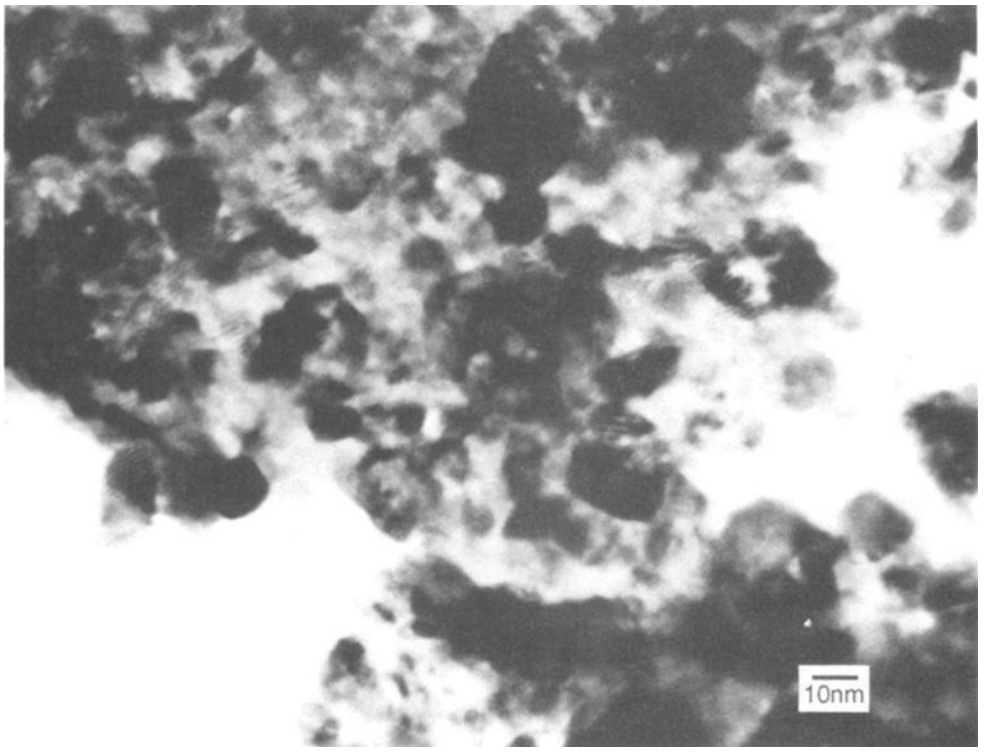

Fig. 3. High resolution micrograph of a ceria-C sample.

a ceria-C sample which had been reduced in a TPR-run as described above. After the reduction, the sample was held at 550°C in flowing He for 10 min. The gas feed was then switched to a stream of helium saturated with H_2O at 0°C. Fig. 4 shows the result of this experiment, compared to an equivalent run with an oxidised sample, for which no reaction with water was expected. The slow increase in the H_2O signal after switching valves is partially due to the adsorption of water on the walls of the unheated tubing connecting the reactor to the mass spectrometer. Nevertheless the curves clearly show that the H_2O signal increases at a later time with the reduced sample, and that H_2 is formed. This finding must be interpreted as the oxidation of Ce^{+III} by water according to

$$CeO_{2-x} + xH_2O \rightleftharpoons CeO_2 + xH_2 . \quad (4)$$

The oxidation proceeds rapidly in the first 100–200 s of contact with water, when the top layers of the ceria are involved. It slows down later, probably due to diffusion phenomena in the bulk of the ceria.

3.2.2. Reoxidation at room temperature

Reoxidation at room temperature was studied by XPS. For these measurements a different preparation method for the oxygen-deficient ceria was used, in order to make the effects more visible. Cerium(III) carbonate was decomposed in a vacuum of less than 10^{-4} mbar at 500°C for 15 min. This treatment leads to a mixed cerium(III/IV) oxide. Pure Ce_2O_3 cannot be formed during the decomposition because Ce^{+III} in the oxide lattice is such a strongly reducing material that it reduces some of the CO_2 evolved to CO and even to elemental carbon [10]. The

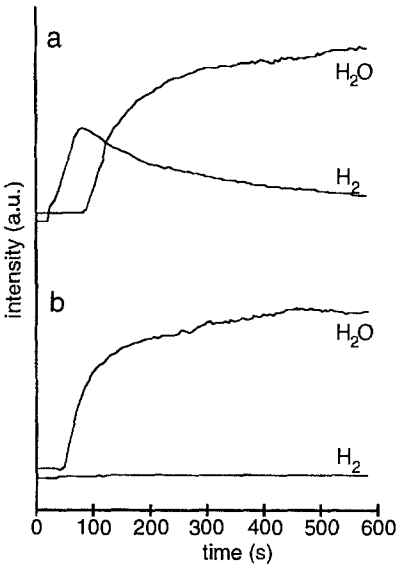

Fig. 4. Reaction of water with ceria-C at 550°C, (a) CO-reduced sample, (b) oxidised sample. He-flow: 40 ml/min, saturation with water at 0°C. Detected gases: H_2 ($m/e = 2$) and H_2O ($m/e = 18$).

highly oxygen deficient ceria obtained by this method was treated with very low partial pressures of water and finally completely reoxidised through contact with air for 5 h. Fig. 5 shows the XPS Ce 3d region of the carbonate, the decomposition product and the products of the subsequent oxidations.

The 3d spectra of Ce^{+III} and Ce^{+IV} exhibit complicated features due to shake-up and shake-down processes which have been extensively investigated both theoretically and experimentally [11–13]. For a qualitative determination of Ce^{+III} versus Ce^{+IV} it is sufficient to recognise that strong peaks at $E_B = 886.2$ eV and $E_B = 904.7$ eV, labelled with v′ and u′ respectively, are typical for Ce(III) while the main features of Ce(IV) are at $E_B = 883.2$ (v), 889.2 (v″), 899.1 (v‴), 901.2 (u), 908.2 (u″), and 917.3 eV (u‴). For quantitative determinations of the Ce^{+IV}/Ce^{+III} ratio, the method proposed by Shyu et al. [14] was used. These authors found that, after subtraction of a non-linear Shirley type background, the ratio of the area of the u‴ peak to the area of the whole Ce 3d multiplet was linearly correlated to the ratio $Ce^{+IV}/(Ce^{+III} + Ce^{+IV})$. Since the values obtained using this method depend on the exact choice of the baseline, their accuracy is estimated to about ±5%. Results from such calculations on the spectra of fig. 5 are summarized in table 2.

The spectrum of the cerium carbonate reveals that about 40% of the near surface cerium is already present as Ce^{+IV}, most probably due to surface oxidation of car-

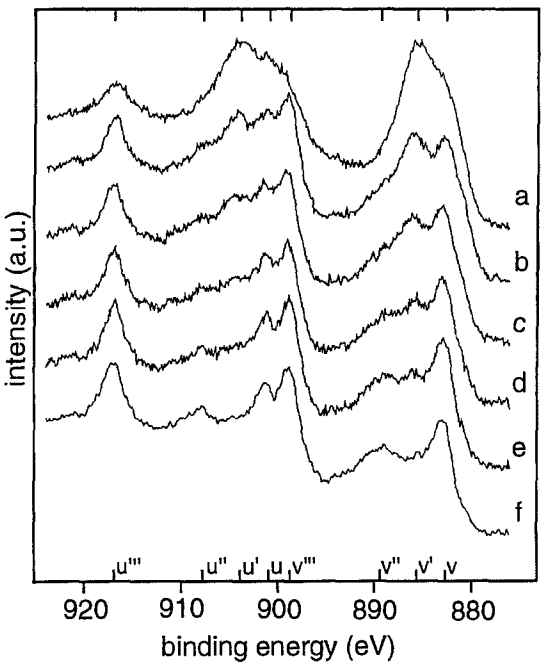

Fig. 5. Ce 3d XPS spectra: (a) cerium(III) carbonate as received; (b) following decomposition in vacuum; (c)–(f): following exposure to 5×10^{-5} Torr H_2O for 30 s (c), 2×10^{-4} Torr H_2O for 1 min (d), 4×10^{-4} Torr H_2O for 5 min (e), and air for 5 h (f).

Table 2
Ratio $Ce^{+IV}/(Ce^{+III} + Ce^{+IV})$ on the surface of different samples determined from the contribution of the u''' peak to the XPS Ce 3d multiplet

Sample	Characterization	% v'''	% Ce^{+IV}
ref.	ceria (Aldrich)	13.0	100
ref.	ceria (literature [14])	13.2	100
ref.	cerium(III) oxalate hydrate (Aldrich)	0	0
a	cerium(III) carbonate (Aldrich)	5.4	41
b	a, decomposed in vacuum, 500°C	7.3	56
c	b, dosed with 5×10^{-5} Torr H_2O, 30 s	8.3	63
d	c, dosed with 2×10^{-4} Torr H_2O, 1 min	9.6	73
e	d, dosed with 4×10^{-4} Torr H_2O, 5 min	11.3	86
f	e, oxidised in air, 5 h, room temperature	13.3	100

bonate, hydroxide or oxide species. After decomposition in vacuum, the Ce^{+IV} content at the surface rises to about 56%, due to oxidation by departing CO_2. This ceria still shows a much higher oxygen deficiency than could be obtained by reduction of CeO_2 in H_2 at 500°C.

The first dosing with 5×10^{-5} Torr H_2O for 30 s leads to oxidation of about 16% of the remaining Ce^{+III}. Stepwise oxidation with further water vapour is indicated in the spectra from the rise in relative intensity of the u, u''', v and v''' peaks, the development of the u'' and v'' features, and the loss of relative intensity in the region of v' and u'. About 70% of the Ce^{+III} present after decomposition of the carbonate was oxidised by the four treatments with water, with the partial pressure of water during the final treatment still being more than 10^5 times lower than in car exhaust gases. Total oxidation to CeO_2 was observed after contact with air for 5 h. The Ce 3d spectrum of this sample is in close agreement with that of pure CeO_2 and the quantification indicates 100% Ce^{+IV}.

3.2.3. Reduction/reoxidation cycles

Since only reversible reduction/oxidation processes can account for the oxygen storage capacity of a catalyst, experiments were performed with conditions cycled between reducing and oxidising, with and without water being present. A stream of 35 ml/min of He, either dry or water-saturated at 0°C, into which 5 ml/min 5% H_2/Ar or 5% O_2/He was added, was passed over 240 mg of ceria-C at constant temperature. Cycle times were 6 min for reduction and 4 min for oxidation. Fig. 6 shows some of the reduction/reoxidation cycles at different temperatures.

At 450°C both the H_2 and the O_2 signal very quickly reach a steady level after switching, indicating that hardly any reduction or oxidation takes place during each cycle. The amounts of water detected were insignificant in this case.

At 550°C with a dry gas feed, a considerable amount of both H_2 or O_2 was consumed after changing gas streams. Water was produced during the reducing step

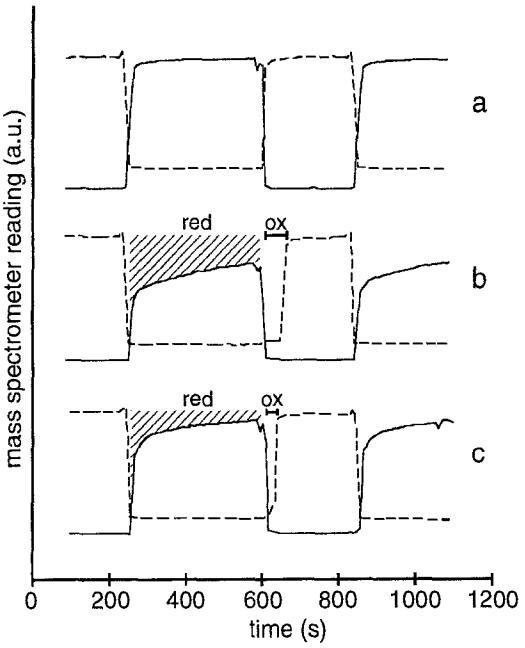

Fig. 6. Reduction/reoxidation cycles with 240 mg ceria-C. (a) 450°C in dry gas feed; (b) 550°C in dry gas feed; (c) 550°C in water saturated gas feed. Gas flow: 40 ml/min, 0.625% O_2 or H_2 in He. Detected gases: (——) H_2 ($m/e = 2$), and (– – –) O_2 ($m/e = 32$).

but, due to a poor signal to noise ratio and problems with adsorption on the walls of the tubing, these values are not included in fig. 6. The way in which H_2 or O_2 is consumed appears to be different. H_2 is consumed over an elongated period of time with a dropping reaction rate (area "red" in fig. 6b), which is typical for diffusion controlled solid-state–gas reactions. Either diffusion of oxide ions to the surface of the particles, diffusion of H_2 into the particles, or diffusion of water formed could be the rate determining step. During oxidation on the other hand, the available O_2 is totally consumed from the moment of switching until reoxidation is complete ("ox" in fig. 6b). This finding indicates a very rapid reaction, which on the time-scale resolved in our experiment appears to be only determined by the amount of oxygen present. Quantification of the consumption of H_2 and O_2 indicates that about 2.5% of the ceria is reversibly reduced.

The ratio of reduction is significantly lowered in presence of water, with both a reduction in consumption of hydrogen during the H_2 period ("red" is smaller in fig. 6c than fig. 6b), and a shorter reoxidation time. Sintering due to the presence of water can be excluded as the reason for this behaviour, since the surface area of the sample did not change during the experiment. In addition, about 80% of the initial reducibility was re-established as soon as dry feed gas stream was used again (not shown in fig. 6). The changed thermodynamics in presence of water apparently account for most of the lower reducibility. It is suspected that the reducibility of

ceria is even lower under conditions closer to car exhaust gases, where the partial pressure of water is much higher and the concentration of reducing gases is lower than in our experiments.

4. Conclusions

The reduction of pure ceria by CO or H_2 strongly depends on properties such as specific surface area and crystallinity. The more perfect the fluorite type CeO_2 structure, the more difficult it is to reduce. Reduction/oxidation carried out by cycling between H_2 and O_2 indicate different kinetics for the two reactions. While reduction appears to be diffusion-controlled, oxidation is very rapid and, on the time-scale investigated, limited only by the amount of oxygen available.

Water will reoxidise reduced ceria with evolution of hydrogen. This occurs at room temperature as well as at elevated temperature, even with low partial pressures of H_2O. Water significantly lowers the rate of ceria reduction by H_2 because the thermodynamic conditions for reduction are changed when water is present.

From these findings we conclude that the influence of water on the reduction behaviour and oxygen storage capacities of ceria-containing catalysts may be significant. This conclusion may not extend to car exhaust catalysts in that the thermodynamics of pure and supported or doped ceria may be different. However, the findings indicate that the influence of water should no longer be neglected in determinations of oxygen storage capacities of such catalysts.

Acknowledgement

This work was supported by the Swiss National Science Foundation. Thanks to Viera Piegerova for the electron microscopic studies.

References

[1] B. Harrison, A.F. Diwell and C. Hallett, Platinum Metals Rev. 32 (1988) 73.
[2] A.F. Diwell, R.R. Rajaram, H.A. Shaw and T.J. Truex, in: *Catalysis and Automotive Pollution Control II*, ed. A. Crucq (Elsevier, Amsterdam, 1991) p. 139.
[3] F. Le Normand, L. Hilaire, K. Kili, G. Krill and G. Maire, J. Phys. Chem. 92 (1988) 2561.
[4] G. Kim, Ind. Eng. Chem. Prod. Res. Dev. 21 (1982) 267.
[5] H.C. Yao and Y.F. Yu Yao, J. Catal. 86 (1984) 254.
[6] E.C. Su, C.N. Montreuil and W.G. Rothschild, Appl. Catal. 17 (1985) 75.
[7] B.K. Cho, J. Catal. 131 (1991) 74.
[8] G. Brauer, K.A. Gingerich and U. Holtschmidt, J. Inorg. Nucl. Chem. 16 (1960) 77.
[9] M.F.L. Johnson and J. Moori, J. Catal. 103 (1987) 502.
[10] C. Padeste, N.W. Cant and D.L. Trimm, in preparation.

[11] A. Fujimori, Phys. Rev. B 28 (1983) 2281.
[12] G. Praline, B.E. Koel, R.L. Hance, H.-I. Lee and J.M. White, J. Electron Spectry. Rel. Phenom. 21 (1980) 21.
[13] F. Le Normand, J. El Fallah, L. Hilaire, P. Légaré, A. Kotani and J.C. Parlebas, Solid State Commun. 71 (1989) 885.
[14] J.Z. Shyu, K. Otto, W.L.H. Watkins, G.W. Graham, R.K. Belitz and H.S. Gandhi, J. Catal. 114 (1988) 23.